Ultrasensitive and highly selective fluorescence probe of nitrogen-doped graphene quantum dots and zinc oxide decorated carbon foam incorporated molecularly imprinted polymer for trace sparfloxacin determination

Nutnicha Chansud[a], Ratirat Kaewnok[a], Piyaluk Nurerk[b], Frank Davis[c], Opas Bunkoed[a]*

[a]Center of Excellence for Innovation in Chemistry, Division of Physical Science, Faculty of Science, Prince of Songkla University, Hat Yai, Songkhla 90110, Thailand

[b]Functional Materials and Nanotechnology Center of Excellence, School of Science, Walailak University, Nakhon Si Thammarat 80160, Thailand

[c]Dept of Engineering and Allied Design University of Chichester, Chichester, PO21 1HR, United Kingdom

Corresponding: Opas Bunkoed, Ph.D.

E-mail: opas.b@psu.ac.th

Abstract

A fluorescent probe was fabricated for the determination of sparfloxacin. The nanocomposite probe was constructed by incorporating nitrogen-doped graphene quantum dots, zinc oxide decorated carbon foam and magnetite into a matrix formed from a molecularly imprinted polymer. The fabricated nanoprobe was characterized and the fabrication and determination conditions were optimized to obtain the highest sensitivity. The determination of sparfloxacin was based on the decreasing of emission response of the nanocomposite probe when the target analyte rebinds to the inherent recognition sites of the fluorescent probe. Under the best conditions, the quenching of fluorescence was linear in the range of 0.10 to 100.0 μg L^{-1} (R^2 = 0.991) with the limit of detection being 0.10 μg L^{-1}. The nanocomposite probe exhibited high specificity with an imprinting factor of 7.93. This optosensor was used to determine sparfloxacin in milk and good recoveries were observed ranging from 93.0 to 100.8 % with RSDs lower than 5%. The results also agreed with the results obtained using a chromatographic method but the developed method has higher sensitivity, at lower cost and faster determination procedure. In addition, the developed optosensor can be simply modified for highly selective determination of other trace levels of target compounds by changing the template with minor changes in determination conditions.

Keywords; Sparfloxacin, nitrogen-doped graphene quantum dots, fluorescence, zinc oxide, carbon foam, selective polymer

1. Introduction

Sparfloxacin is a fluoroquinolone drug having a broad spectrum of antibacterial action which is commonly used in poultry, livestock and aquaculture for anti-infective therapy [1, 2]. Sparfloxacin residue can be accumulated in meat, eggs and dairy products which can lead to detrimental effects on consumer health such as bacterial resistance to antibiotics or raise the risk of allergic reaction. The European Union has set the maximum residual limit (MRL) for sparfloxacin at 50 μg L^{-1} [1]. Therefore, it is necessary to develop a highly sensitive and selective analytical method for the determination of trace sparfloxacin in food samples.. A variety of analytical techniques have been reported to determine sparfloxacin including capillary electrophoresis [2], high performance liquid chromatography [3] and enzyme-linked immunosorbent assay [4]. These techniques generally require expensive equipment, skilled technicians and time-consuming sample preparation procedures. These constraints led to increased interest in the spectrofluorimetry method due to its simplicity, rapidity and low cost. For trace analysis of sparfloxacin in complicated sample matrices, the sensitivity and selectivity of the analytical method need to be improved. The enhancement of sensitivity of spectrofluorimetry method can be achieved using analyte specific material incorporated in a composite sensing probe. Due to a good optical properties, quantum dots has attracted increasing attention and has been widely used as sensitive fluorescent probe for the detection of various target analytes at trace levels. Fluorescent sensing probes based on QDs were developed for the determination of sparfloxacin including thiol-capped CdSe/CdS QDs [5], hydrophilic silica-functionalized CdTe quantum dots (SQDs) [6], thioglycolic acid-modified $CuInS_2$ QDs [7]. Graphene quantum dots (GQDs), a zero-dimensional substance, have recently gained popularity in the field of fluorescence sensing due to their great photostability, biocompatibility, and low toxicity [8]. GQDs with a few atomic layer graphene sheets can exhibit strong photoluminescence (PL) [9]. According to previous reports, GQDs may be

efficiently tuned by doping materials with heteroatoms to modify their unique properties, such as optical characteristics, and surface features. Nitrogen-doped graphene quantum dots (N-GQDs) can be readily doped into the graphene structure via C–N bonds because nitrogen atoms not only has an atomic size equivalent to carbon, but can also form strong bonds with carbon atoms due to its five valence electrons [10]. N-GQDs have been employed as sensitive fluorescent probes for trace determination of organic compounds such as thiosulfate anion and oxidative compounds [11] and warfarin [12].

The lack of selectivity of the spectrofluorimetric method for the determination of sparfloxacin can be improved using molecularly imprinted polymers (MIPs) as a highly specific sensing material. MIPs have a considerably broader set of benefits including great plasticity, ease of production, high selectivity with the target analyte and low cost [13]. MIPs are normally synthesized with a template, monomers and a cross-linker [14]. The functional groups for the recognition sites are produced by the monomers interacting with the template molecule. After copolymerization supported by cross-linking is followed by effective template removal, particular recognition sites with shape, size and functional groups complementary to the template are formed [15]. Due to the availability of binding sites, the target molecule could be rebound with high specificity [16]. In addition, the binding rate and adsorption capacity of the analyte to the sensing probe can be enhanced by the addition of affinity material into the composite probe [17]. Zinc oxide (ZnO) decorated with carbon foam, as a carrier of molecular imprinting sites, is an attractive material with a large geometric surface for the adsorption of target analyte via π-π interaction and hydrogen bonding [18]. Furthermore, using magnetic nanoparticles (Fe_3O_4) to modify the sensing probe is an interesting method of incorporating their attractive properties, as well as additional benefits [19]. In the nanohybrid sensing probe, magnetic nanoparticles can be employed to preconcentrate or enrich target analytes.

In this work, an N-GQDs-MIP-ZnO/CF-Fe_3O_4 nanocomposite probe was developed and used as a highly sensitive and selective sensing probe for the first time for the determination of sparfloxacin. The template imprinting technique was used to produce N-GQDs-MIP-ZnO/CF-Fe_3O_4 sensing probes, which used sparfloxacin as templates, N-GQDs as a sensing material and ZnO/CF as an affinity material, whilst Fe_3O_4 was utilized for simple preconcentration of the target analyte. The optical properties and selective fluorescence response characteristics of N-GQDs-MIP-ZnO/CF-Fe_3O_4 sensing probe were examined. In optimum condition, the N-GQDs-MIP-ZnO/CF-Fe_3O_4 sensing probe displayed a high selective fluorescence quenching ability towards sparfloxacin. Furthermore, using the N-GQDs-MIP-ZnO/CF-Fe_3O_4 sensing probe, a fluorescence optosensor was constructed and effectively employed in the determination of trace sparfloxacin in food samples.

2. Experimental

2.1. Chemical and materials

Sparfloxacin (≥ 99%) was from LGC Ltd (UK). Tetraethyl orthosilicate (TEOS, ≥ 99%) was from Tokyo Chemical Industry Co. Ltd (Tokyo, Japan). 3-aminopropyl triethoxysilane (APTES, ≥ 98%), citric acid (≥ 99%), $FeCl_2.4H_2O$ (≥ 99%) and $FeCl_3.6H_2O$ (≥ 99%) were from Sigma-Aldrich (MO, USA). Tris (hydroxymethyl) aminomethane (Tris-HMA, ≥ 99%), ammonia (NH_3, 25%), sodium hydroxide (NaOH, ≥ 98%) and ethanol (≥ 99%) were from RCI Labscan (Bangkok, Thailand). Dialysis bags (Cut-off 12-14 kD) were from Spectrum Laboratories, Inc. (CA, USA). Disodium hydrogen orthophosphate dodecahydrate ($Na_2HPO_4{\cdot}12H_2O$, ≥99%) was from Univar (Ajax Finechem, Australia).

2.2. Instrumental

Fluorescence measurements were performed using a Cary eclipse fluorescence spectrophotometer (Agilent Technologies, USA). UV-Vis spectra were recorded with a UV-2600i UV-Vis Spectrophotometer (Shimadzu, Japan). Field emission scanning electron

microscopy (FESEM) (Apreo FEI, Netherlands) was used to observe the morphology of the nanocomposite probes and related materials. FTIR spectra were recorded using a Fourier transform infrared spectrometer (Bruker, Germany). Raman spectrum of N-GQDs was recorded using a Raman Microscope Spectrometer (RAMANforce, Nanoproton, Japan). The energy dispersive X-ray (EDS) spectrum was produced with an Energy Dispersive Spectrometer (Oxford Instruments, England).Zeta potentials were achieved by Zeta potential analyzer (Model Zeta PALS, Brookhaven, USA.

2.3. Preparation of magnetite nanoparticles (Fe_3O_4)

Co-precipitations of $FeCl_2.4H_2O$ and $FeCl_3.6H_2O$ were conducted to prepare Fe_3O_4 nanoparticles which were slightly modified from previous work [20]. Firstly, 1.10 g of $FeCl_2.4H_2O$ and 3.00 g of $FeCl_3.6H_2O$ were dissolved in 150 mL of deionized water (DI) and then heated to 70 °C under vigorous agitation to obtain a yellow solution. Then, ammonia solution was added dropwise and vigorously stirred for 1 h at 80 °C under N_2 gas. The obtained Fe_3O_4 particles were collected by an external magnet and washed with 50 mL of DI for three times. Finally, the Fe_3O_4 nanoparticles were then dried at 80 ˚C for 6 h.

2.4. Synthesis of nitrogen-doped graphene quantum dots (N-GQDs)

In a round-bottom flask, citric acid (2.00 g) were mixed with 0.50 g of Tris-HMA and heated at 220 °C for 10 min. The formation of N-GQDs occurred with a solid orange product appearing. Then, 5.0 mL of DI was added to the synthesized N-GQDs and 0.25 M NaOH was added to neutralize the solution to pH 7.0 [21].

2.5. Synthesis of zinc oxide carbon foam (ZnO/CF)

The synthesis of ZnO/CF was modified from a previous work [22]. In a beaker, 3.00 g of sucrose and 1.50 g of $Zn(NO_3)_2{\cdot}6H_2O$ were mixed and heated at 110 °C for 10 min under stirring. The color of the mixture turned to black, indicating the formation of carbon foam.

2.6. Synthesis of N-GQDs-MIP-ZnO/CF-Fe_3O_4

The synthesis of the N-GQDs-MIP-ZnO/CF-Fe_3O_4 probe commenced with the mixing of 10 mg of sparfloxacin, 5.0 mL of N-GQDs (21.0 mg L^{-1}), and 5.0 mL of DI in a 30 mL brown bottle. The mixture was stirred for 30 min. 180 µL of APTES were added and stirring continued for further 60 min. Subsequently, 260 µL of TEOS, 5.0 mg of Fe_3O_4, 60 mg of ZnO/CF and 200 µL of NH_3 (25%) were added to the mixture solution and stirred for 90 min. The synthesized nanocomposite probes were separated using a magnet. Finally, the template (sparfloxacin) was removed by washing with 10 mL of ethanol for three times. The removal of template from the probe was checked by measuring sparfloxacin in washing solution using UV–Vis spectrophotometry. The composite non-imprinted polymer probe was prepared under the same condition with composite MIP probe but without adding of the template (sparfloxacin). The synthesis procedure of N-GQDs-MIP-ZnO/CF-Fe_3O_4 is illustrated in **Fig. 1.**

2.7. Determination condition

The nanocomposite N-GQDs-MIP-ZnO/CF-Fe_3O_4 and N-GQDs-NIP-ZnO/CF-Fe_3O_4 probes (1.0 mg mL^{-1}) were dispersed in phosphate buffer at pH 7.0, 300 µL of the dispersion was mixed with 2.0 mL of standard or sample solution and incubated for 18 min. Then, the nanocomposite probe with adsorbed sparfloxacin was isolated using a magnet and dispersed in 100 µL phosphate buffer before determination. The analysis was performed using excitation at 330 nm. Fluorescence emissions were measured from 360 to 700 nm (a slit width of 10 nm). The analysis was performed at 25 °C for simple and convenient procedure. The results were reported as mean ± standard deviation which was conducted by Excel software.

2.8. Sample pretreatment of milk

Milk samples were simply pretreated to remove fat and protein before analysis with the developed method. A 10.0 mL sample of milk was centrifuged at 5000 rpm for 10 min to remove fat. Then, acetonitrile (10 mL) was added into the defatted milk and vortexed for 1

min. The mixture was centrifuged at 5000 rpm for 5 min. The supernatant was evaporated to dryness at 60 °C and redissolved with 10.0 mL of DI water. The pretreated milk samples were mixed with the developed N-GQDs-MIP-ZnO/CF-Fe_3O_4 sensing probe and the determination carried out as described in **section 2.7**.

2.9. The determination of sparfloxacin using HPLC method

The HPLC condition for the analysis of sparfloxacin is provided in Supporting Information.

3. Results and Discussion

3.1. Characterization of the nanocomposite sensing probe and related materials

The functional groups of the nanocomposite sensing probe and related materials were investigated by FTIR technique (**Fig. S1**). The FTIR spectra of N-GQDs (**Fig. S1a**) showed the absorption peaks at 766, 1006, 1188, 1542 and 1735 cm^{-1} which correspond to epoxy group vibration, C-H bending, C-O stretching, C=C stretching and C=O vibration, respectively. The characteristic peak at 2980 cm^{-1} related to C-H stretching and the broad band at 3436 cm^{-1} is due to the –OH and –NH stretching [21, 23]. FTIR spectra of ZnO/CF (**Fig. S1b**) showed the characteristic peaks at 1076, 1404 and 1598 cm^{-1} due to Zn-O-C bond, -OH bending and C=C stretching, respectively. Absorption peak at 2924 cm^{-1} was due to C-H stretching and 3384 cm^{-1} corresponding to –OH stretching [24]. In the spectra of Fe_3O_4-SiO_2-NH_2 (**Fig. S1c**), the peaks were appeared at 444 (Si-O stretching), 519 (Fe-O stretching), 1399 (Fe-O stretching), 1624 (bending vibration of absorbed water) and 3422 cm^{-1} (-OH/-NH stretching) [18]. The absorption peaks of N-GQDs, ZnO/CF and Fe_3O_4-SiO_2-NH_2 are also appeared in the FTIR spectra of composite N-GQDs-MIP-ZnO/CF-Fe_3O_4 sensing probe (**Fig. S1d**). These spectra confirm that all related materials were successfully incorporated into the MIP to form the nanocomposite sensing probe. Raman spectrum of the synthesized N-GQDs **(Fig. S2)** showed an obvious disordered D band at around 1384 cm^{-1} and a crystalline G band at about 1541 cm^{-1}

which indicated the intercalation of N atoms into the conjugated carbon backbone of GQDs [25].

The surface morphologies of N-GQDs, ZnO/CF and N-GQDs-MIP-ZnO/CF-Fe_3O_4 were investigated using TEM and SEM techniques. **Fig. 2A and B** illustrated TEM images of N-GQDs and N-GQDs-MIP-ZnO/CF-Fe_3O_4 sensing probe. **Fig. 2C and D** showed the SEM images of ZnO/CF and N-GQDs-MIP-ZnO/CF-Fe_3O_4 sensing probe. ZnO/CF showed a high porosity, while the nanocomposite sensing probe exhibited a rough surface due to the presence of the produced recognition sites for sparfloxacin. The MIP sensing probe exhibited a particle size of about 300 nm **(Fig. S3)**. The BET surface areas of N-GQDs-MIP-ZnO/CF-Fe_3O_4 was higher than those of the N-GQDs-NIP-ZnO/CF-Fe_3O_4 sensing probes, being 14.246 m^2g^{-1} and 6.249 m^2g^{-1}, respectively. The average pore size of N-GQDs-MIP-ZnO/CF-Fe_3O_4 and N-GQDs-NIP-ZnO/CF-Fe_3O_4 were 17.67 nm and 12.36 nm, respectively. These results were also confirmed that the recognition cavities are produced on the MIP sensing probe. Adsorption and desorption isotherms of N-GQDs-MIP-ZnO/CF-Fe_3O_4 and N-GQDs-NIP-ZnO/CF-Fe_3O_4 sensing probes are showed in **Fig. 2E and 2F**, respectively. In addition, the chemical composition in the nanocomposite sensing probe was analyzed using energy dispersive X-ray spectroscopy (EDS) and the results indicated that N-GQDs-MIP-ZnO/CF-Fe_3O_4 was successfully prepared (**Fig. S4**). The template removal procedure was investigated to ensure that all template molecules were completely removed from the composite sensing probe before applying it to determine sparfloxacin in real sample. The fluorescence emission of composite sensing probe exhibited low response in the presence of template and restored as the same level of non-MIP after removing the template (**Fig. 3**). These results can confirm that all template molecule were successfully removed from the composite sensing probe which can be used to determine target analyte in real samples without the memory effect.

The quantum yield (QY) of N-GQDs and N-GQDs-NIP-ZnO/CF-Fe_3O_4 were determined using quinine sulfate (QY=54%) as the fluorescence standard reference [25]. The QY of the as-prepared N-GQDs and N-GQDs-NIP-ZnO/CF-Fe_3O_4 were calculated to be 68.6% and 22.3%, respectively. These results implied that N-GQDs had good optical properties for optosensing applications.

3.2. Optimization of composite sensing nanoprobe fabrication and determination conditions

The conditions for the determination of sparfloxacin utilizing the N-GQDs-MIP-ZnO/CF-Fe_3O_4 sensing probe were evaluated and optimized to achieve the highest sensitivity with the shortest analysis time. The effect of binding time between sparfloxacin and the sensing probe, effect of amount of ZnO/Carbon foam, effect of template to monomer to cross-linker ratios and effect of pH of dispersion solution were investigated and optimized. The change in emission intensity (F_0/F) was used to evaluate the proper binding time, while other parameters were evaluated based on the sensitivity of the optosensor. The sensitivity was obtained from the slope of the calibration curve which was plotted between F_0/F and sparfloxacin concentration ranging from 0.10 to 100.0 μg L^{-1}.

3.2.1. Effect of binding time between sparfloxacin and sensing probe

The binding time between sparfloxacin and N-GQDs-MIP-ZnO/CF-Fe_3O_4 sensing probe was evaluated from 2 to 30 min. The quenching efficiency (F_0/F) improved as the binding time increased from 2 to 18 min (**Fig. 4A**), and then remained practically constant. As a result, 18 min of binding time was chosen as optimal to determine sparfloxacin using N-GQDs-MIP-ZnO/CF-Fe_3O_4 sensing probe.

3.2.2. Effect of amount of ZnO/Carbon foam (ZnO/CF)

The amounts of ZnO/CF used to produce the composite N-GQDs-MIP-ZnO/CF-Fe_3O_4 sensing probe were investigated in a range from 30 mg to 80 mg. The results revealed that 60

mg exhibited the best sensitivity (**Fig. 4B**). Low sensitivity was obtained when 30 mg of ZnO/CF was used which may be attributed to a weak affinity between sparfloxacin and the sensing probe. When the amount of ZnO/CF increased to 70 mg, however, the sensitivity was also reduced. This was due to excess ZnO/CF disrupting the creation of specific recognition sites within the sensing probe, resulting in reduced sensitivity. As a result, 60 mg of ZnO/CF was used to fabricate the sensing probe.

3.2.3. Effect of template (TP) to monomer (MN) to cross-linker (CL)

The amount of TP, MN and CL used to synthesize MIP affects the creation of recognition sites which in turn affects the sensitivity of the probe toward the target analyte. The mole ratio of the TP-MN was evaluated at 1: 25, 1:30 and 1:35. The ratio of the TP-CL was evaluated at 1:40, 1:45 and 1:50. Sensitivity was low at a TP-MN ratio at 1:25 because the probe presented fewer -NH_2 groups to bind with the sparfloxacin. At a TP-MN ratio of 1:35, on the other hand, excess monomer disrupted the formation of recognition sites and non-specific binding increased. The lower mole ratio of CL (1:40) produced a weak MIP layer with low sensitivity, whereas the higher mole ratio of CL (1:50) disrupted the formation of recognition sites. The sensitivity of the composite sensing probe was the highest at a TP- MN-CL mole ratio of 1: 30: 45 (**Fig. 4C**) and this ratio was chosen as the best condition for the preparation of the composite sensing probe.

3.2.4. Effect of dispersion solution pH

The effect of dispersion solution pH on the fluorescence quenching of the composite sensing probe for the determination of sparfloxacin were evaluated by adjusting the pH of the dispersion solution with a phosphate buffer from pH 5.0 to 8.0 (**Fig. 4D**). The fluorescence quenching of the nanocomposite probe by sparfloxacin increased from pH 5.0 to 7.0 and then decreased from pH 7.0 to 8.0. With lower or higher pH, the sensitivity loss attributed to amine protonation in acidic and the carboxylic acid ionization in alkaline environments, both of which

induce structural damage to the recognition cavities in the silica shell, resulting in a low sensitivity for the determination of sparfloxacin. Therefore, the N-GQDs-MIP-ZnO/CF-Fe_3O_4 probe was dispersed in phosphate buffer at pH 7.0 before analysis of the sample solution.

3.3. Comparison of different nanocomposite sensing probes

Various nanocomposite probes were evaluated for their sensitivity toward sparfloxacin. The probes evaluated were an N-GQDs-NIP-Fe_3O_4 probe, an N-GQDs-NIP-ZnO/CF-Fe_3O_4 probe, an N-GQDs-MIP-Fe_3O_4 probe and an N-GQDs-MIP-ZnO/CF-Fe_3O_4 probe. The nanocomposite N-GQDs-MIP-ZnO/CF-Fe_3O_4 probe exhibited the highest sensitivity (**Fig. 5**) due to the presence of both specific recognition sites for sparfloxacin and ZnO/CF which enhanced the adsorption of sparfloxacin on the sensing probe. While, N-GQDs-NIP-Fe_3O_4 sensing probe provided the lowest sensitivity due to the absence both of recognition sites and ZnO/CF, only non-specific interaction occurred between sensing probe and sparfloxacin. This study confirmed the suitability of the N-GQDs-MIP-ZnO/CF-Fe_3O_4 probe for the determination of sparfloxacin in real samples.

3.4. Analytical performance

The analytical performance of the developed optosensor was evaluated including linearity, limit of detection (LOD), limit of quantification (LOQ) and imprinting factor. Under the optimum condition, the intensity of N-GQDs-MIP-ZnO/CF-Fe_3O_4 fluorescence decreased linearity from analyte concentrations from 0.10 to 100.0 μg L^{-1}, R^2 = 0.991. **Fig. 6A and B** demonstrated the emission spectra of the N-GQDs-MIP-ZnO/CF-Fe_3O_4 and N-GQDs-NIP-ZnO/CF-Fe_3O_4 nanoprobes in the presence of various concentration of sparfloxacin. **Fig. 6C and D** showed the calibration curves of N-GQDs-MIP-ZnO/CF-Fe_3O_4 and N-GQDs-NIP-ZnO/CF-Fe_3O_4 nanoprobes for the determination of sparfloxacin. The LOD and LOQ were 0.10 and 0.35 μg L^{-1} which were determined based on 3SD/Slope and 10SD/Slope, respectively. The imprinting factor was determined from the ratio of sensitivity of MIP and

NIP nanocomposite to be 7.93. These results imply that the developed sensing probes contain specific recognition sites to specifically rebind with sparfloxacin.

The quenching mechanism of the N-GQDs-MIP-ZnO/CF-Fe_3O_4 probe can be explained according to the Stern – Volmer equation, $F_0/F = 1+K_{sv}[C]$, where F_0 and F are the emission response in the absence and presence of sparfloxacin, respectively, and C and K_{sv} are the sparfloxacin concentration and the quenching constant, respectively. Normally, the fluorescence quenching of quantum dots is either an electron or an energy transfer mechanism [26]. In the present work, there was no spectral overlap between the absorption spectrum of sparfloxacin and the emission spectrum of the N-GQDs-MIP-ZnO/CF-Fe_3O_4 probe (**Fig. S5**). Therefore, the energy transfer quenching mechanism is not possible [27]. Sparfloxacin shows an absorption band from 200 to 400 nm, which overlapped with the excitation spectrum of the N-GQDs-MIP-ZnO/CF-Fe_3O_4 probe. Thus, the fluorescence quenching mechanism was an electron transfer process. The zeta potential of the N-GQDs-MIP-ZnO/CF-Fe_3O_4 probe was 6.38 mV, indicating that the positive charges surface. The zeta potential of N-GQDs-MIP-ZnO/CF-Fe_3O_4 probe in the presence of sparfloxacin was -26.45 mV, indicating that hydrogen bonding interaction occurred between N-GQDs-MIP-ZnO/CF-Fe_3O_4 probe and sparfloxacin. When sparfloxacin bound with recognition sites of the nanocomposite probe, the electrons of N-GQDs were excited from the ground state to an excited state. In the absence of sparfloxacin around the N-GQDs-MIP-ZnO/CF-Fe_3O_4 probe, the excited electrons of N-GQDs returned to the valence band whilst producing fluorescence. Whereas, in the presence of sparfloxacin, the NH_2 groups of APTES interact with carbonyl groups of sparfloxacin via hydrogen bonding. Electron transfer occurred from the high energy band of orbitals in the conduction band of N-GQDs to the lowest unoccupied molecular orbital of sparfloxacin. The transfer of electrons from the N-GQDs to sparfloxacin quenched fluorescence [28, 29, 30].

3.5. Stability and Reproducibility

The stability of the N-GQDs-MIP-ZnO/CF-Fe_3O_4 nanocomposite probe was determined in a buffer solution at pH 6.0, 7.0 and 8.0. The sensing probe was extremely stable, the fluorescence intensity was not changed appreciably after storing the sensing probe in buffer solution for 350 min (**Fig. S6A**), which is ample time for spectrofluorimetry investigation. To investigate the reproducibility of the N-GQDs-MIP-ZnO/CF-Fe_3O_4 sensing probe, six different probes which were synthesized at different times (n=6) under optimum conditions. The RSDs of average sensitivity were 1.90%. These results revealed a high level of reproducibility (**Fig. S6B**).

3.6. Selectivity and competitive study

One of the most important criteria of an analytical procedure is selectivity. The recognition ability and selectivity of the N-GQDs-MIP-ZnO/CF-Fe_3O_4 and N-GQDs-NIP-ZnO/CF-Fe_3O_4 sensing probe were compared using chemical structural analogs of sparfloxacin including marbofloxacin, ciprofloxacin, lomefloxacin, ofloxacin, levofloxacin and other antibiotics (ampicillin, cefazolin, cefoperazone, sulfadimethoxine) and calcium ion. The fluorescence quenching of the N-GQDs-MIP-ZnO/CF-Fe_3O_4 sensing probe demonstrated a great sensitivity toward sparfloxacin and a much lower sensitivity to their chemical structural analogs and other compounds, as shown in **Fig. 7A**. The N-GQDs-NIP-ZnO/CF-Fe_3O_4 sensing probe exhibited similar fluorescence quenching on exposure to sparfloxacin and the analogs. These results indicated that the functional bases on the N-GQDs-NIP-ZnO/CF-Fe_3O_4 sensing probe were disorganized and that specialized recognition sites were not present. To confirm the selectivity of the developed sensing probe, a competitive study was performed. Sparfloxacin was detected in the presence of various amounts of ofloxacin using the N-GQDs-MIP-ZnO/CF-Fe_3O_4 sensing probe (**Fig. 7B**). According to these results, the N-GQDs-MIP-ZnO/CF-Fe_3O_4 sensing probe demonstrated higher selectivity for sparfloxacin than ofloxacin. The N-GQDs-MIP-ZnO/CF-Fe_3O_4 sensing probe exhibited more binding sites, and the

sparfloxacin could be strongly bound to particular imprinting sites on the N-GQDs-MIP-ZnO/CF-Fe_3O_4 sensing probe surface. Specific fluorescence quenching occurs as a result of this procedure.

3.7. Analysis of sparfloxacin in milk samples

The developed N-GQDs-MIP-ZnO/CF-Fe_3O_4 probe was utilized to determine sparfloxacin in milk. Low concentrations of sparfloxacin were found in some samples, but lower than the MRL. The accuracy of the fabricated sensing probe was further evaluated by analyzing milk samples spiked with standard sparfloxacin at 1.0, 10.0, 50.0 and 75.0 μg L^{-1}. Good recoveries were achieved in the range of 93.0 to 100.8%, with RSDs of less than 2.8% (**Table 1**). This result confirmed that the developed method is accurate and can be utilized to determine sparfloxacin in food samples. The inter-day and intra-day precision of the developed optosensor were also evaluated in real samples. The inter-day was performed by determining sparfloxacin over five days (n=5) and intra-day was performed within one day (n=6). The RSDs were calculated to be 4.8% for inter-day precision and 3.5% for intra-day precision. The developed strategy has a good precision for the determination of sparfloxacin in milk samples.

3.8. Comparison with HPLC method

The developed optosensor was compared with a HPLC technique for the determination of sparfloxacin in milk. The chromatograms of spiked milk at various concentrations of sparfloxacin are shown in **Fig. 8A**. The results of the optosensor were consistent with the HPLC technique, with a R^2 of 0.9981 (**Fig. 8B**). As a result, the optosensor based on the N-GQDs-MIP-ZnO/CF-Fe_3O_4 sensing probe can be used as an accurate and precise determination of sparfloxacin. In addition, when compared with other previous works (**Table 2**), the developed optosensor has lower LOD than reported in other works which implied that the developed method is suitable for trace analysis. The accuracy in term of recovery and precision are better or comparable with other works. Upon consideration of instrument requirements and solvent

consumption, the developed optosensor used a simple, rapid, cost-effective instrument, small amount of solvents and do not require expert operators. However the liquid chromatographic method required more expensive instruments and used much larger amounts of organic solvent for the mobile phase composition. Therefore, it can be concluded that the developed strategy can be utilized as a highly sensitive and selective method for the determination of trace levels of sparfloxacin in food samples.

4. Conclusion

An optosensor was successfully developed for the determination of trace sparfloxacin in milk. The optosensor was fabricated based on a nanocomposite probe by incorporating N-GQDs, ZnO/CF and Fe_3O_4 nanoparticles into a selective polymer matrix. The nanocomposite probe exhibited high sensitivity and good selectivity for sparfloxacin with a high imprinting factor. The developed optosensor has a high accuracy, achieving relative recoveries between 93.0 and 100.8%. Analysis results were in good agreement those obtained with a chromatographic method, however, the developed optosensor has several advantages over the chromatographic method such as speed, low toxic solvent consumption, convenience and higher sensitivity. The developed strategy can be potentially adapted to determine other compounds in complex matrix sample, although some important parameters may be need to be optimized for a range of target compounds.

Acknowledgments

This work was supported by the Faculty of Science Research Fund (SCIEQUIP65001). The authors would like to acknowledge the Center of Excellence for Innovation in Chemistry (PERCH-CIC), the Ministry of Higher Education, Science, Research and Innovation. Nutnicha Chansud was supported by PSU-Ph.D. Scholarship, Graduate School, Prince of Songkla University, Contract no. PSU_PHD2564-01. The authors thank Mr. Thomas Duncan Coyne for English proofreading.

Table 1. The determination of sparfloxacin in milk samples using the N-GQDs-MIP-ZnO/CF-Fe_3O_4 sensing probes (*n*=3).

Milk samples	Sparfloxacin (μg L^{-1})		Recovery (%)	RSD (%)
	Added	Found		
I	0.0	-	-	-
	1.0	0.96	99.80	2.52
	10.0	9.79	98.31	1.52
	50.0	46.48	93.03	1.84
	75.0	74.27	99.08	0.97
II	0.0	0.32	-	-
	1.0	1.32	99.3	1.4
	10.0	9.83	95.1	2.1
	50.0	48.26	95.9	1.4
	75.0	74.13	98.4	2.3
III	0.0	-	-	-
	1.0	0.90	97.7	2.3
	10.0	9.53	96.1	0.8
	50.0	47.26	94.7	2.8
	75.0	73.87	98.6	2.0
IV	0.0	0.06	-	-
	1.0	0.99	93.0	2.6
	10.0	9.52	94.6	1.7
	50.0	50.48	100.8	0.9
	75.0	75.42	100.5	1.6

Table 2. A comparison of analytical performances produced by various methods for the determination of sparfloxacin

Method	Sample	Linearity ($\mu g\ kg^{-1}$ or $\mu g\ L^{-1}$)	LOD ($\mu g\ kg^{-1}$ or $\mu g\ L^{-1}$)	Recovery (%)	RSD (%)	References
LC/MS	Rat plasma	10-1000	2	96.2-110.9	10.2-10.4	[31]
ELISA	Rat plasma	5-2000	5	87.7-106.2	4.8-15.3	[4]
RP-HPLC	Pharmaceutical	5000-25000	573	98.0-99.1	0.3-1.7	[3]
CE	Tap water, river water, honey, milk, Yogurt	20-3200	<10	87.8-110.2	1.2-6.3	[32]
Fluorescence (B-CQDs)	Water, milk	0.59-51.01	0.20	96.0-103.5	1.8-2.9	[1]
UPLC-MS/MS	Egg	2-500	0.4	78.3-84.4	2.3-4.6	[33]
Fluorescence (CdSe/CdS QDs)	Milk	500-30000	139.1	95.3-106.8	1.42	[5]
Photoluminescent (SQDs)	Human serum	19.6-78482	19.6	84.0-95.6	1.25-5.38	[6]
Fluorescence ($CuInS_2$ QDs)	Pharmaceutical	500-1000000	500	97.6-103.8	1.2	[7]
Optosensor N-GQDs-MIP-ZnO/CF-Fe_3O_4 probe	Milk	0.10-100.0	0.10	93.0-100.8	< 5	This work

LC/MS = Liquid chromatography/Mass spectrometry, ELISA = Enzyme-linked immunosorbent assay, RP-HPLC= Reversed-phase high performance liquid chromatography, CE= Capillary electrophoresis, MS/MS = Tandem mass spectrometry and UPLC = Ultra-performance liquid chromatography

References

[1] H.R.H. Ali, A.I. Hassan, Y.F. Hassan, M.M. El-Wekil, Mannitol capped magnetic dispersive micro-solid-phase extraction of polar drugs sparfloxacin and orbifloxacin from milk and water samples followed by selective fluorescence sensing using boron-doped carbon quantum dots, J. Environ. Chem. Eng. 9(2) (2021) 105078. https://doi.org/10.1016/j.jece.2021.105078.

[2] K. Yu, M.-E. Yue, J. Xu, T.-F. Jiang, Determination of fluoroquinolones in milk, honey and water samples by salting out-assisted dispersive liquid-liquid microextraction based on deep eutectic solvent combined with MECC, Food Chem. 332 (2020) 127371. https://doi.org/10.1016/j.foodchem.2020.127371.

[3] N. Jain, D.R. Jain, D. Jain, V. Patel, S. Jain, Development and validation of a green bioanalytical method for the determination of sparfloxacin in pharmaceutical dosage form and human plasma by RP-HPLC, Int. Res. J. Pharm. 9 (2016) 193-202. https://doi.org/10.7897/2230-8407.07671.

[4] H.-J. Zeng, R. Yang, B. Liu, L.-F. Lei, J.-J. Li, L.-B. Qu, Simple and sensitive determination of sparfloxacin in pharmaceuticals and biological samples by immunoassay, J. Pharm. Anal. 2 (2012) 214–219. https://doi.org/10.1016/j.jpha.2012.02.001.

[5] M. Hou, X. Yan, L. Xiong, Determination of sparfloxacin with CdSe/CdS quantum dots as fluorescent probes, J. Lumin. 157 (2015) 58-62. https://doi.org/10.1016/j.jlumin.2014.08.006.

[6] D. Li, S. Jia, E. Fodjo, H. Xu, C. Kong, Y. Wang, Highly sensitive “Turn-on” Fluorescence probe for the detection of sparfloxacin in human serum using silica-functionalized CdTe quantum dots, RSC Adv. 5 (2015). https://doi.org/10.1039/C5RA21587K.

[7] J. Fang, B. Dong, Y. Fu, D. Tang, Detection of sparfloxacin based on water-soluble $CuInS_2$ quantum dots, Results Chem. 2 (2020) 100027. https://doi.org/10.1016/j.rechem.2020.100027.

[8] P. Tian, L. Tang, K.S. Teng, S.P. Lau, Graphene quantum dots from chemistry to applications, Mater. Today Chem. 10 (2018) 221-258. https://doi.org/10.1016/j.mtchem.2018.09.007.

[9] Z. Fan, S. Li, F. Yuan, L. Fan, Fluorescent graphene quantum dots for biosensing and bioimaging, RSC Adv. 5(25) (2015) 19773-19789. https://doi.org/10.1039/C4RA17131D.

[10] L. Zhang, D. Peng, R.-P. Liang, J.-D. Qiu, Nitrogen-doped graphene quantum dots as a new catalyst accelerating the coordination reaction between cadmium (II) and 5,10,15,20-tetrakis(1-methyl-4-pyridinio)porphyrin for cadmium(ii) sensing, Anal. Chem. 87(21) (2015) 10894-10901. https://doi.org/10.1021/acs.analchem.5b02450.

[11] Y. Wang, Y. Hu, W. Weng, S. Chang, H. Xu, D. Li, D. Li, Nitrogen-doped graphene quantum dots based fluorescent probe for highly sensitive detection of thiosulfate anion and oxidative compounds, J. Photochem. Photobiol. A: Chem. 412 (2021) 113234. https://doi.org/10.1016/j.jphotochem.2021.113234.

[12] P. Li, Y. Du, M. Ma, J. Zhang, Nitrogen-doped graphene quantum dots coated with molecularly imprinted polymers as a fluorescent sensor for selective determination of warfarin, New J. Chem. 46(16) (2022) 7537-7544. https://doi.org/10.1039/D2NJ00853J.

[13] N. Assi, L. Nejdl, K. Zemankova, K. Pavelicova, J. Bezděková, M. Macka, V. Adam, M. Vaculovicova, UV-induced Zn:Cd/S quantum dots in-situ formed in the presence of thiols for sensitive and selective fluorescence detection of thiols, Sci. Rep. 11 (2021) 13806. https://doi.org/10.1038/s41598-021-93137-4.

[14] M. Nurrokhimah, P. Nurerk, P. Kanatharana, O. Bunkoed, A nanosorbent consisting of a magnetic molecularly imprinted polymer and graphene oxide for multi-residue analysis of cephalosporins, Microchim. Acta 186 (2019) 822. https://doi.org/10.1007/s00604-019-3985-5

[15] A.M.L. Piloto, D.S.M. Ribeiro, S.S.M. Rodrigues, J.L.M. Santos, P. Sampaio, G. Sales, Imprinted fluorescent cellulose membranes for the on-site detection of myoglobin in biological media, ACS Appl. Bio Mater. 4(5) (2021) 4224-4235. https://doi.org/10.1021/acsabm.1c00039.

[16] B. Li, J. Xu, A.J. Hall, K. Haupt, B. Tse Sum Bui, Water-compatible silica sol–gel molecularly imprinted polymer as a potential delivery system for the controlled release of salicylic acid, J. Mol. Recognit. 27(9) (2014) 559-565. https://doi.org/10.1002/jmr.2383.

[17] N. Orachorn, O. Bunkoed, Nanohybrid magnetic composite optosensing probes for the enrichment and ultra-trace detection of mafenide and sulfisoxazole, Talanta 228 (2021), 122237. https://doi.org/10.1016/j.talanta.2021.122237

[18] A. Kliangsuwan, A. Phonchai, O. Bunkoed, A magnetic molecularly imprinted polymer hierarchical composite adsorbent embedded with a zinc oxide carbon foam nanocomposite for the extraction of sulfonamides, Microchem. J. 179 (2022) 107443. https://doi.org/10.1016/j.microc.2022.107443.

[19] X. Li, L. Chen, Fluorescence probe based on an amino-functionalized fluorescent magnetic nanocomposite for detection of folic acid in serum, ACS Appl. Mater. Interfaces 8(46) (2016) 31832-31840. https://doi.org/10.1021/acsami.6b10163.

[20] O. Bunkoed, P. Raksawong, R. Chaowana, P. Nurerk, A nanocomposite probe of graphene quantum dots and magnetite nanoparticles embedded in a selective polymer for the enrichment and detection of ceftazidime, Talanta 218 (2020) 121168. https://doi.org/10.1016/j.talanta.2020.121168.

[21] Y. Liu, N. Cao, W. Gui, Q. Ma, Nitrogen-doped graphene quantum dots-based fluorescence molecularly imprinted sensor for thiacloprid detection, Talanta 183 (2018), 339–344. doi:10.1016/j.talanta.2018.01.063

[22] M. Sajid, C. Basheer, M. Mansha, Membrane protected micro-solid-phase extraction of organochlorine pesticides in milk samples using zinc oxide incorporated carbon foam as sorbent, J. Chromatogr. A 1475 (2016) 110-115.
https://doi.org/10.1016/j.chroma.2016.11.008.

[23] L. Zhang, J. Wang, G. Fang, J. Deng, S. Wang, A molecularly imprinted polymer capped nitrogen-doped graphene quantum dots system for sensitive determination of tetracycline in animal-derived food, Chemistry Select 5(2) (2020) 839-846.
https://doi.org/10.1002/slct.201903868.

[24] S. Khongkla, A. Phonchai, P. Nurerk, O. Bunkoed, A hierarchical composite ZnO@Carbon foam/PVA cryogel sorbent for the extraction and enrichment of parabens and synthetic phenolic antioxidant in fruit juice, Microchem. J. 173 (2022) 107013. https://doi.org/10.1016/j.microc.2021.107013.

[25] L. Lin, M. Rong, S. Lu, X. Song, Y. Zhong, J. Yan, Y. Wang, X. Chen, A facile synthesis of highly luminescent nitrogen-doped graphene quantum dots for the detection of 2,4,6-trinitrophenol in aqueous solution, Nanoscale, 7 (2015) 1872-1878.
https://doi.org/10.1039/C4NR06365A

[26] X. Bi, L. Li, L. Luo, X. Liu, J. Li, T. You, A ratiometric fluorescence aptasensor based on photoinduced electron transfer from CdTe QDs to WS_2 NTs for the sensitive detection of zearalenone in cereal crops, Food Chem. 385 (2022) 132657 https://doi.org/10.1016/j.foodchem.2022.132657.

[27] Z. Gan, X. Hu, X. Xu, W. Zhang, X. Zou, J. Shi, K. Zheng, M. Arslan, A portable test strip based on fluorescent europium-based metal-organic framework for rapid and visual detection of tetracycline in food samples, Food Chem. 354 (2021) 129501. https://doi.org/10.1016/j.foodchem.2021.129501.

[28] S. Huang, L. Tan, L. Zhang, J. Wu, L. Zhang, Y. Tang, H. Wang, Y. Liang, Molecularly imprinted mesoporous silica embedded with perovskite $CsPbBr_3$ quantum dots for the fluorescence sensing of 2,2-dichlorovinyl dimethyl phosphate, Sens. Actuators B: Chem. 325 (2020) 128751. https://doi.org/10.1016/j.snb.2020.128751.

[29] M. Amjadi, R. Jalili, Molecularly imprinted mesoporous silica embedded with carbon dots and semiconductor quantum dots as a ratiometric fluorescent sensor for diniconazole, Biosensors and Bioelectronics, 96 (2017) 121-126. https://doi.org/10.1016/j.bios.2017.04.045

[30] W. Zhu, Y. Zhou, S. Liu, M. Luo, J. Du, J. Fan, H. Xiong, H. Peng, A novel magnetic fluorescent molecularly imprinted sensor for highly selective and sensitive detection of 4-nitrophenol in food samples through a dual-recognition mechanism, Food Chemistry, 348 (2021) 129126. https://doi.org/10.1016/j.foodchem.2021.129126

[31] K. Noh, K.-I. Kwon, T. Jeong, W. Kang, Quantitative determination of sparfloxacin in rat plasma by liquid chromatography/tandem mass spectrometry, Biomed. Chromatogr. 24 (2010) 1199-202. https://doi.org/10.1002/bmc.1427.

[32] J. Yu, L. Huan, Y. Wang, J. Li, D. Wu, X. Wang, Fluorescent sensing system based on molecularly imprinted phase-change microcapsules and carbon quantum dots for high-efficient detection of tetracycline, J. Colloid Interface Sci. 599 (2021). https://doi.org/10.1016/j.jcis.2021.04.094.

[33] X. Xu, W. Zhao, B. Ji, Y. Han, G. Xu, M. Jie, N. Wu, Y. Wu, J. Li, K. Li, D. Zhao, Y. Bai, Application of silanized melamine sponges in matrix purification for rapid multi-residue analysis of veterinary drugs in eggs by UPLC-MS/MS, Food Chem. 369 (2022) 130894. https://doi.org/10.1016/j.foodchem.2021.130894.

Fig. 1. The synthesis process of the nanocomposite N-GQDs-MIP-ZnO/CF-Fe_3O_4 sensing probe for the determination of sparfloxacin

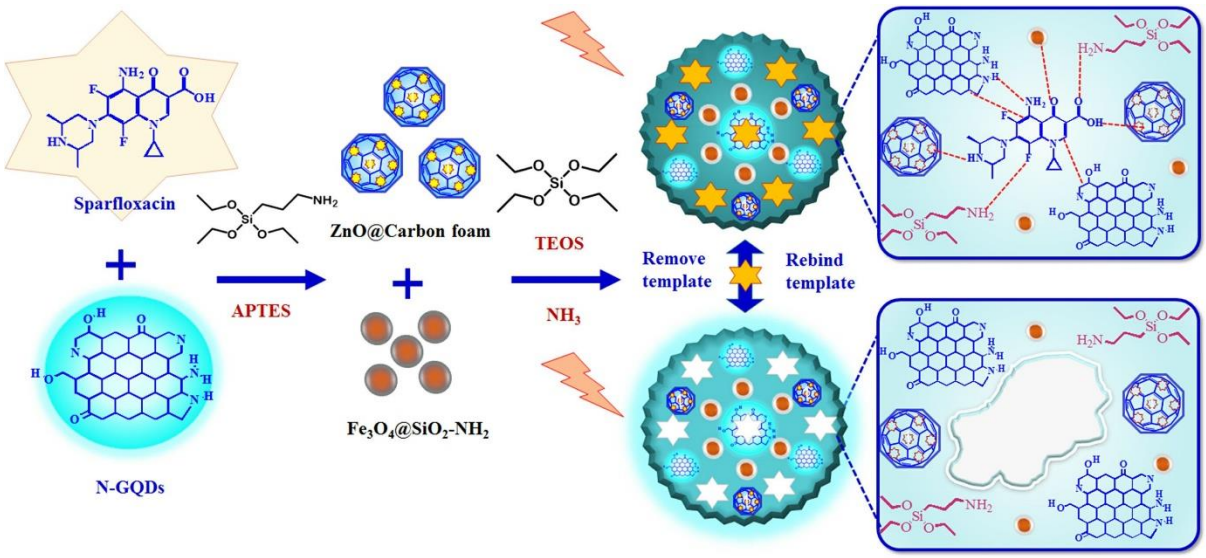

Fig. 2. TEM images are of N-GQDs (A) and N-GQDs-MIP-ZnO/CF-Fe_3O_4 (B). SEM images are of ZnO/CF (C), and N-GQDs-MIP-ZnO/CF-Fe_3O_4 at 25,000X (D). The adsorption and desorption isotherms are of the N-GQDs-MIP-ZnO/CF-Fe_3O_4 (E) and N-GQDs-NIP-ZnO/CF-Fe_3O_4 sensing probes (F)

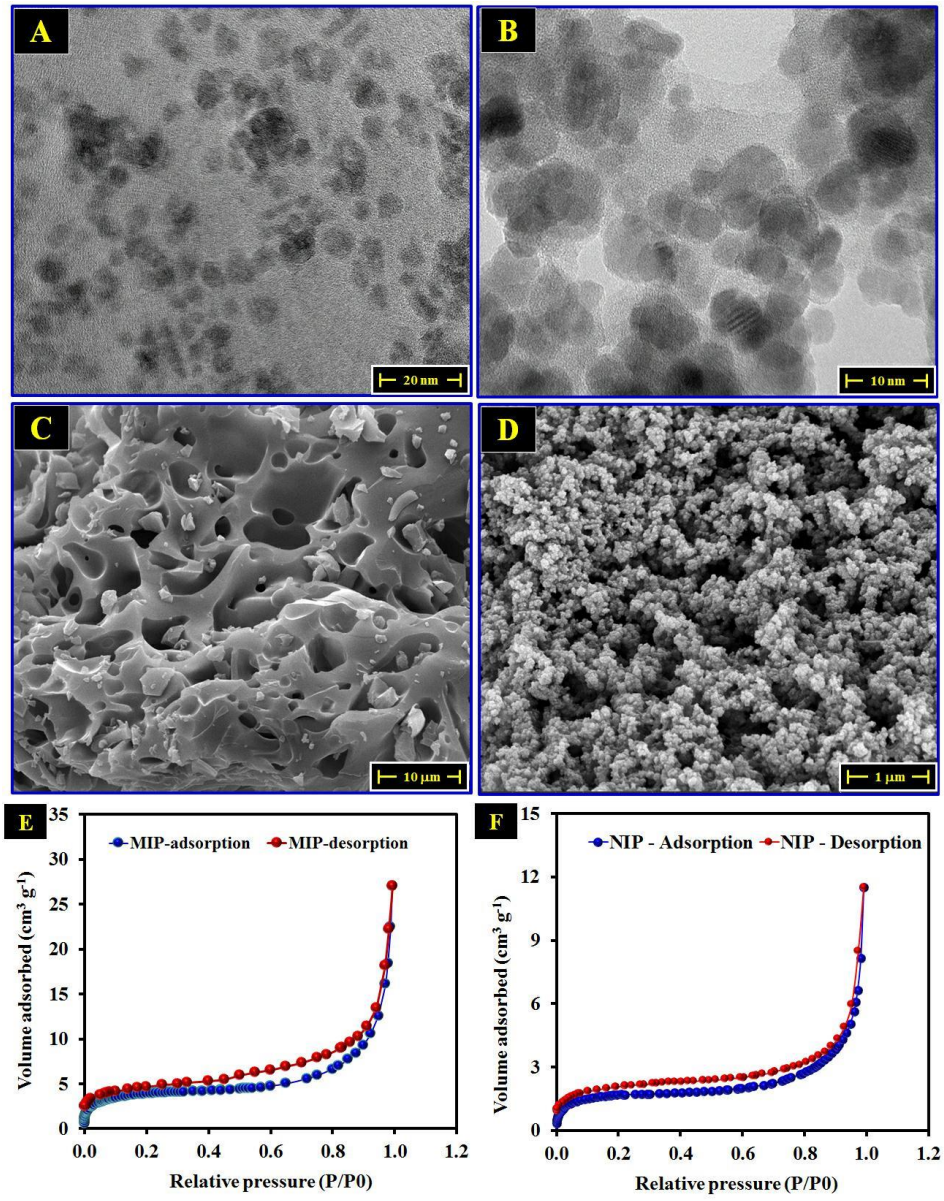

Fig. 3. Fluorescence emission spectra of N-GQDs-MIP-ZnO/CF-Fe_3O_4 before removal of template (a), N-GQDs-MIP-ZnO/CF-Fe_3O_4 after removal of template (b) and N-GQDs-NIP-ZnO/CF-Fe_3O_4 sensing probe (c)

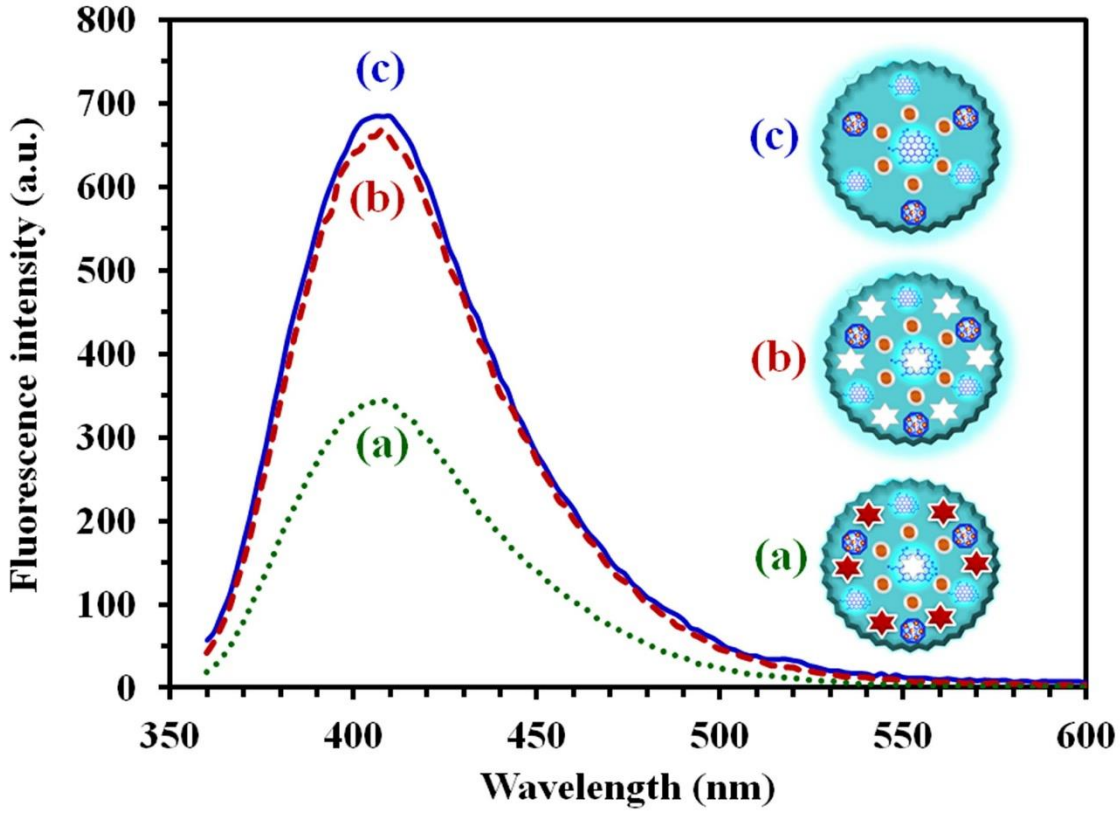

Fig. 4. Effect of binding time between sparfloxacin and N-GQDs-MIP-ZnO/CF-Fe_3O_4 sensing probe (A), effect of amount of ZnO/Carbon foam (B), effect of template to monomer to cross-linker (C) and effect of pH of dispersion solution (D) on the sensitivity of the developed optosensor for the determination of sparfloxacin. Error bars represent standard deviation of 3 replicate measurements (*n*=3).

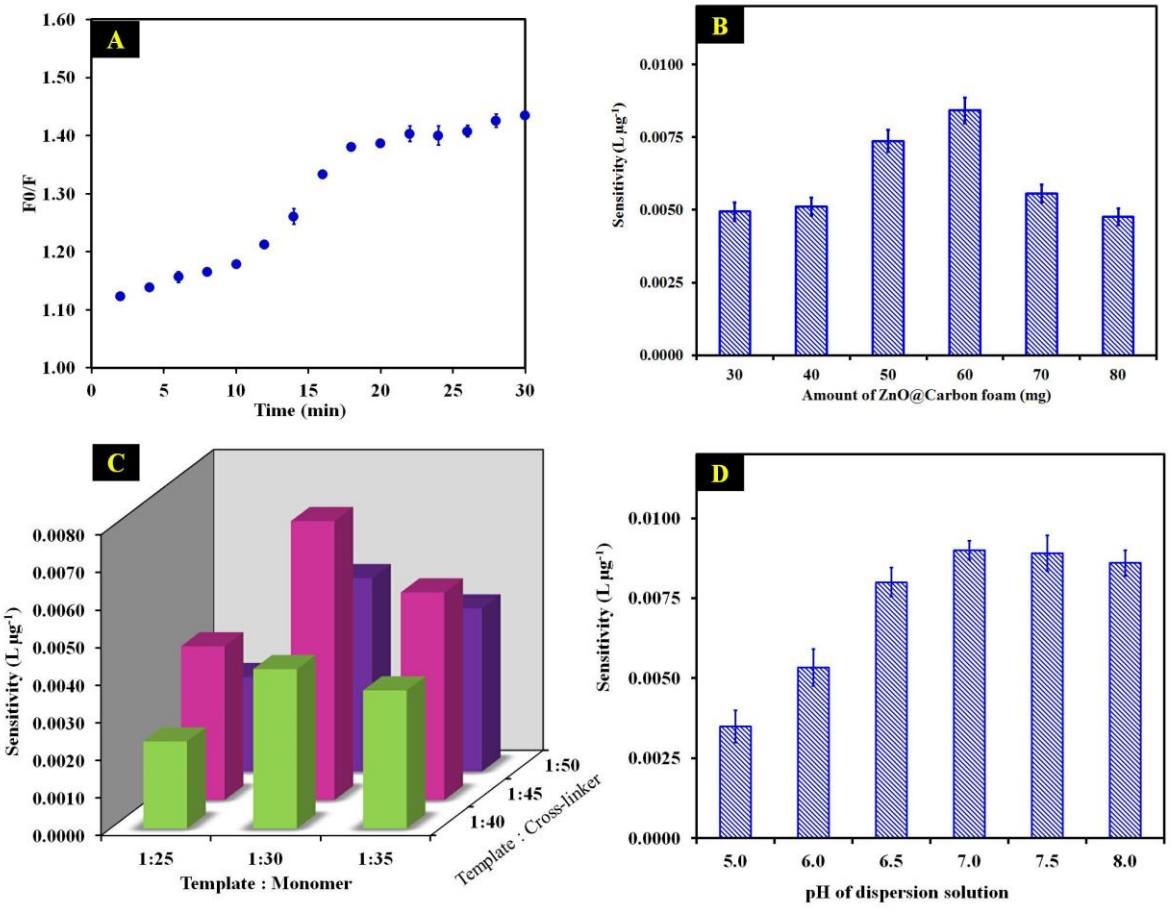

Fig. 5. The chart shows the sensitivity of various nanocomposite sensing probes toward sparfloxacin (Error bars represent standard deviation of 3 replicate measurements; *n*=3). (N-GQDs = nitrogen-doped quantum dots; NIP = non-imprinted polymer; CF = carbon foam; MIP = molecularly imprinted polymer)

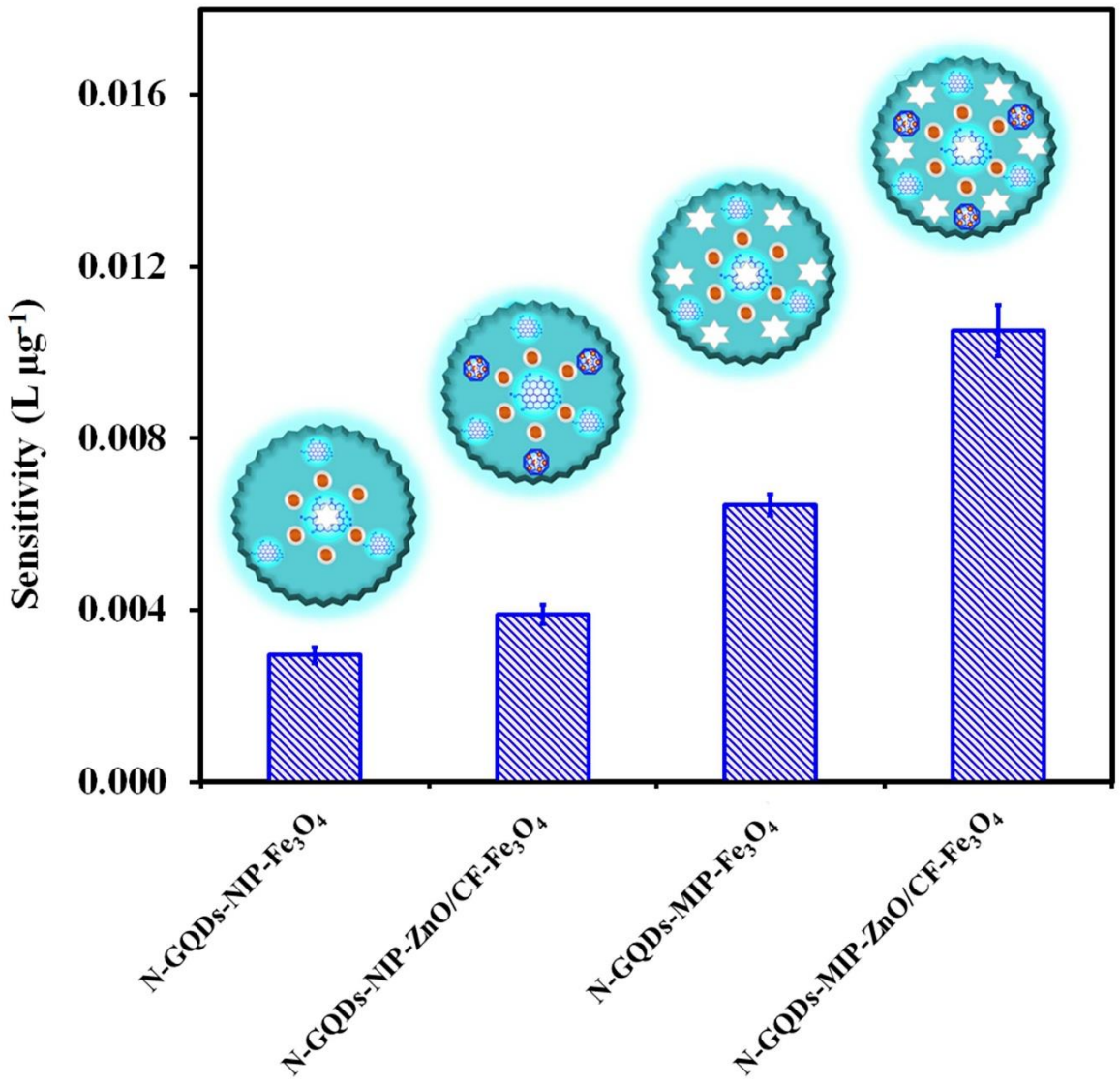

Fig. 6. The fluorescence emission spectra of the N-GQDs-MIP-ZnO/CF-Fe_3O_4 sensing probe (A) were produced in various concentration of sparfloxacin; in set is the photograph of sensing probe without sparfloxacin (left) and in the presence of sparfloxacin at 100.0 μg L^{-1} (right). The fluorescence emission spectra (B) were produced by the N-GQDs-NIP-ZnO/CF-Fe_3O_4 sensing probe in various concentrations of sparfloxacin. The calibration curves of the N-GQDs-MIP-ZnO/CF-Fe_3O_4 (C) and N-GQDs-NIP-ZnO/CF-Fe_3O_4 (D) were plotted for the determination of sparfloxacin. Error bars represent standard deviation of 3 replicate measurements (*n*=3).

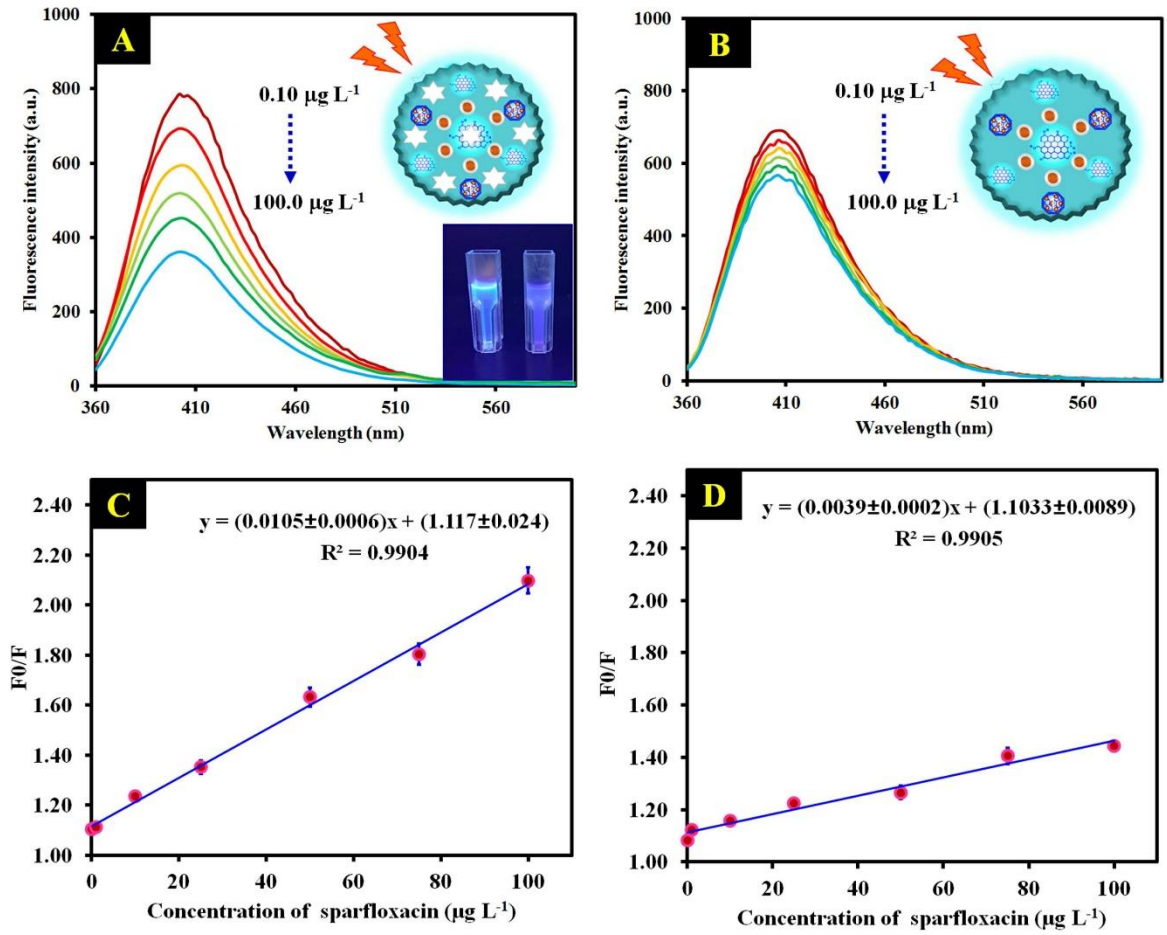

Fig. 7. The selectivity study (A) of the N-GQDs-MIP-ZnO/CF-Fe_3O_4 sensing probe toward sparfloxacin included five structural analogs of sparfloxacin, other antibiotics and ion. The competitive study (B) involved sparfloxacin and ofloxacin. Error bars represent standard deviation of 3 replicate measurements (*n*=3).

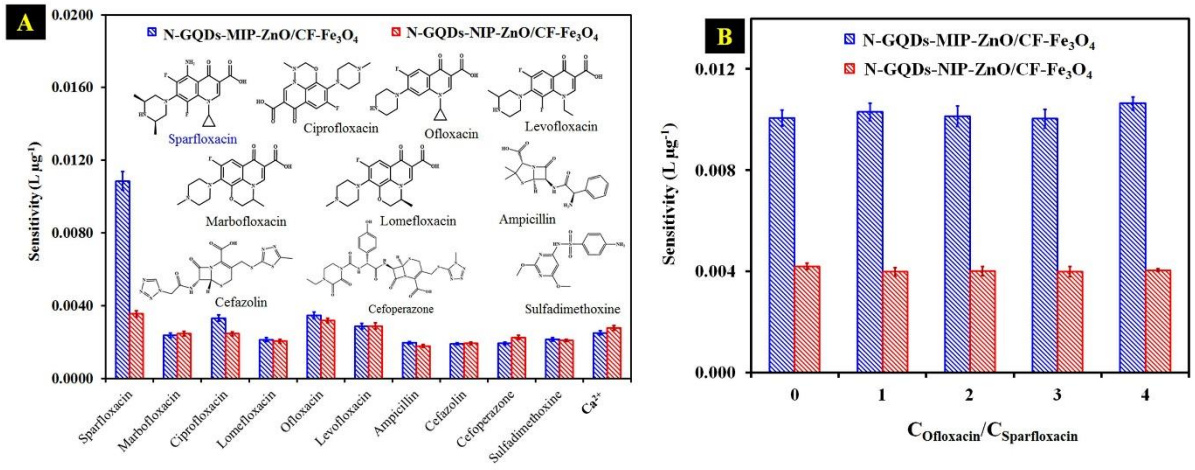

Fig. 8. HPLC chromatogram of spiked milk sample with different concentrations of sparfloxacin (A). The scatterplot compares the results obtained from the determination of sparfloxacin in milk, using the developed optosensor and HPLC (B).